Journal of Catalysis **192,** 307–315 (2000)
doi:10.1006/jcat.2000.2825, available online at http://www.idealibrary.com on IDEAL®

Hydrodesulfurization and Hydrogenation Activities of Alumina-Supported Transition Metal Sulfides

J. Quartararo, S. Mignard, and S. Kasztelan[1]

Kinetics and Catalysis Division, IFP, 1 et 4 Avenue de Bois-Préau, 92852 Rueil-Malmaison Cedex, France

Received September 26, 1999; revised December 17, 1999; accepted January 17, 2000

The catalytic activities of several alumina-supported monometallic sulfides covering a wide range of heats of formation or metal–sulfur bond energies, namely, Mn, Fe, Zn, Cu, Ni, Ru, Mo, and Re sulfides, have been measured for the hydrogenation of cyclohexene, the hydrodesulfurization (HDS) of benzothiophene, and the hydrodesulfurization of dibenzothiophene under typical hydrotreating conditions. For the hydrodesulfurization of dibenzothiophene a volcano curve similar to the one reported for bulk sulfides (Pecoraro, T., and Chianelli, R. R., *J. Catal.* 67, 430 (1981)) is found when the HDS activities are plotted versus the metal–sulfur bond energy, suggesting that the alumina support has no major infuence on the volcano curve. For cyclohexene hydrogenation and benzothiophene HDS different trends are found, suggesting that the activity trends depend on the nature of the reactant and/or reaction. The activities expressed in moles of reactant per mole of sulfided metal of Mn, Fe, Zn, Cu, and Ni sulfides are found to be very low, whereas the activities of Ru, Mo, and Re sulfides are high and of the same order of magnitude. © 2000 Academic Press

INTRODUCTION

The dibenzothiophene hydrodesulfurization (HDS) activity of bulk transition metal sulfides (TMS) has been reported to follow a so-called *volcano* curve when plotted against the heat of formation of the TMS (1). Similar tendencies have been subsequently reported for HDS and other catalytic reactions for bulk as well as carbon-supported sulfides (2–10). On alumina, only a few comparisons of a limited number of metal sulfides, generally noble metal sulfides, have been reported (9–15).

While noble metal sulfide based catalysts are often reported as the most active sulfides, a number of differences can be found in the ranking of catalysts activities depending on the nature of the reactant, the nature of the support, the catalyst activation conditions, and the testing operating conditions. For example, bulk ruthenium sulfide as well as carbon-supported Ru sulfide are very active for dibenzothiophene HDS (1, 3, 4, 16) while this does not always appear to be the case for alumina-supported Ru sulfide (12, 14). For aromatic hydrogenation (HYD) bulk ruthenium sulfide is very active (2, 17), whereas for alumina-supported Ru sulfide a low hydrogenation activity is found (11, 13). For hydrodenitrogenation (HDN), ruthenium sulfide is seldom the best catalyst (5–7, 11, 14, 18–22). Some tests with a real feed have been reported (9, 18, 21) and they led to the conclusion that Ru sulfide is often the most reactive. Among other factors that may influence these results, one major factor appears to be the sulfiding method of the supported ruthenium sulfide (22–28).

It appears therefore that it is not clear whether the shape of the volcano curve reported by Pecoraro and Chianelli (1) depends on the nature of the reactant and the nature of the support. In this work, we have investigated the influence of the nature of the reactant and reaction by measuring the catalytic properties for the hydrogenation of cyclohexene, the HDS of benzothiophene, and the HDS of dibenzothiophene of a set of alumina-supported monometallic sulfide catalysts. The sulfides have been chosen to cover a wide range of heat of formation or preferably metal–sulfur bond energy, namely, Mn, Fe, Zn, Cu, Ni, Ru, Mo, and Re as reported in Table 1 (1, 29, 30). Most of these alumina-supported sulfides have also been chosen because they were expected to be easily sulfided under our experimental conditions. These conditions are typical of the usual hydrotreating processes with a 6 MPa total pressure and a high H_2S partial pressure (about 0.1 MPa). Catalysts were also characterized in their sulfided state by X-ray diffraction (XRD) and transmission electron microscopy (TEM).

EXPERIMENTAL

Catalyst preparation. All catalysts were prepared by pore-filling impregnation of a γ-alumina support (Procatalyse, 263 m^2/g, 0.57 cm^3/g, 1.2-mm extrudates) with aqueous solutions of the following metallic salts: $Fe(NH_4)_3(C_2O_4)_3 \cdot xH_2O$, $Cu(NO_3)_2 \cdot 3H_2O$, $Mn(NO_3) \cdot 4H_2O$, $Zn(NO_3)_2 \cdot 4H_2O$, $Ni(NO_3)_2 \cdot 6H_2O$, $RuCl_3 \cdot H_2O$, $(NH_4)_6Mo_7O_{24} \cdot 4H_2O$, and NH_4ReO_4. For Fe/Al_2O_3, the use of iron nitrate is

[1] To whom correspondence should be addressed. Fax: 33(1) 47 52 60 55. E-mail: slavik.kasztelan@ifp.fr.

0021-9517/00 $35.00

TABLE 1

Metal Loading and BET Surface Area of Fresh Catalysts and Metal–Sulfur Bond Energy of Sulfides

Catalyst	Metal (wt%)	Metal (at/nm^2)[a]	S_{BET} (m^2/g)	ΔH form (kcal/mol) (1)	E^{exp}_{M-S} (kcal/mol) (29, 30)	E^{calc}_{M-S} (kcal/mol) (29, 30)
Mn	5.9	2.6	202	51.0	30.9	23.0
Fe	5.6	2.4	228	24.0	31.8	31.0
Zn	6.2	2.3	213	—	36.5	37.5
Cu	6.3	2.4	226	—	40.2	42.6
Ni	5.6	2.3	202	17.2	41.3	41.5
Ru	7.6	1.9	—	49.2	50.7	51.7
Mo	8.6	2.3	231	65.8	59.7	61.9
Re	10.2	1.4	237	42.7	60.3	62.9

[a] Computed using the alumina BET surface area.

known to lead to a poor distribution of the metal in the alumina grain (31). The same difficulty was also encountered with iron chloride (4). Therefore, we chose a wet impregnation of the alumina support with an aqueous solution of ammonium ferric oxalate. For Re/Al_2O_3 two successive impregnations were needed. For the Ru/Al_2O_3 catalyst three impregnations were needed to deposit the amount of Ru chosen. The wet samples were dried at 120°C overnight and calcined in air at 500°C for 3 h except for the Ru catalyst which was not calcined but only dried at 120°C overnight as recommended in the literature (32). In the following the catalysts will be symbolized by the chemical symbols of the metal deposited on the alumina support, namely Mn, Fe, Zn, Cu, Ni, Ru, Mo, and Re.

The metal contents of the prepared catalysts were measured by X-ray fluorescence and are reported in Table 1. Metal contents were targeted to be 2.5 at. metal/nm^2, except for Ru and Re which were targeted to be at 1.8 and 1.4 at. metal/nm^2, respectively.

Catalytic tests. The catalysts were tested for three different reactions, namely, hydrogenation of cyclohexene (CHE), HDS of benzothiophene (BT), and HDS of dibenzothiophene (DBT) in a continuous flow high-pressure fixed bed "Catatest" unit from VINCI Technologies, France. The conditions used for the catalytic test were a total pressure of 6 MPa, a reaction temperature chosen in the range 250–350°C, a liquid hourly space velocity (LHSV) chosen in the range 1–24 h^{-1}, a ratio $H_2/HC = 450$ L/L (STP), and a volume of 40 cm^3 of catalyst. Prior to catalytic testing, the catalysts were sulfided at 350°C for 2 h. Sulfiding, testing conditions, and feed compositions are summarized in Table 2.

For CHE hydrogenation, the liquid products of the reaction were analyzed by gas chromatography using a 50-m CPsil5 CB column (film thickness, 1.2 μm; internal diameter, 0.32 mm) and a flame ionization detector. Temperature programming of the chromatograph was constant at 40°C for 10 min and then the temperature increases to 280°C at 5°C/min.

Under our experimental conditions the main products from CHE hydrogenation were cyclohexane and two sulfur-containing compounds, namely, cyclohexanethiol and cyclohexane methyl sulfide. Cyclohexanethiol is considered to be obtained from the addition of H_2S to cyclohexene due to the relatively high H_2S partial pressure employed (Table 2). Cyclohexane methyl sulfide is obtained from the reaction of CH_3SH generated from the decomposition of DMDS, employed to generate the H_2S partial pressure with cyclohexanethiol. Therefore, two sets of conversion and activities have been defined, one for CHE transformation ($r_{w,trans}$) and one for CHE hydrogenation ($r_{w,hyd}$), leading to the formation of cyclohexane. The HYD of CHE was found to be a first-order reaction under our conditions, as is usually found in the literature (33–35).

For BT and DBT hydrodesulfurization, the liquid products of the reaction were analyzed by gas chromatography using a 10-m CPsil19 CB column (film thickness, 0.2 μm; internal diameter, 0.25 mm) and a flame ionization detector. Temperature programming of the gas chromatograph was 40°C for 2 min, and then the temperature was increased to 240°C at 25°C/min. The main products from BT HDS were dihydrobenzothiophene and ethylbenzene. Dihydrobenzothiophene is a well-known hydrogenated intermediate prior to desulfurization (33, 34). Two sets of conversion and activities have been defined, one for BT transformation ($r_{w,trans}$) and one for BT true HDS ($r_{w,hds}$), leading to the formation of ethyl benzene. HDS of BT was a first-order reaction under our conditions, as is usually found in the literature (33–35) with an activation energy of 80 kJ/mol (33, 36–38).

TABLE 2

Experimental Conditions for Sulfiding and Catalytic Testing

Conditions	Sulfiding	HYD of CHE	HDS of BT	HDS of DBT
Total pressure (MPa)	6	6	6	6
Temperature (°C)	350	250	250	350
LHSV (h^{-1})	2	1	Variable	Variable
H_2/HC (L/L)	350	450	450	450
	Feed Composition (wt%)			
Cyclohexene	—	10	—	—
Benzothiophene	—	—	3	—
Dibenzothiophene	—	—	—	3
Dimethyldisulfide	2	2	2	2
Cyclohexane	98			
Decaline	—	88	95	95
	Partial Pressures (MPa)			
Decaline		1.34	1.49	1.5
Reactant		0.26	0.05	0.035
Methane		0.09	0.092	0.093
H_2		4.31	4.36	4.37
H_2S		0.09	0.092	0.093

The main products from DBT HDS were tetrahydrodibenzothiophene, biphenyl, and phenylcyclohexane as is well-known (33–35). Two sets of conversion and activities were defined, one for DBT transformation and one for DBT true HDS (formation of biphenyl and phenylcyclohexane). The HDS of DBT has been found to be a first-order reaction in our conditions, as is usually found in the literature with an activation energy of 120 kJ/mol (33, 35, 39, 40).

All conversions were determined in a steady state regime reached generally after 4 h on stream. First-order rates of reaction were computed using the following formulas (33–35):

$$r_w = -\frac{F}{W}\ln(1-X) \quad \text{in mol of reactant/kg of catalyst/h,} \qquad [1]$$

or

$$r_m = -\frac{F}{N}\ln(1-X) \quad \text{in } 10^{-3} \text{ mol of reactant/mol of metal/h,} \qquad [2]$$

or

$$r_{ms} = 100 \cdot r_m/\tau \quad \text{in } 10^{-3} \text{ mol of reactant/mol of metal sulfided/h,} \qquad [3]$$

with F being the reactant molar flow rate (mol/h), W the weight of the catalyst, N the moles of metal loaded in the reactor, and τ the sulfiding degree (%) of the metal.

Used catalysts. The used catalysts recovered after the tests were washed with toluene in a Soxhlet apparatus, stored under purified toluene, and dried before analysis. C and S elemental analysis were performed on a LECO SC-132 apparatus for the sulfur and a CARLO ERBA 1106 apparatus for the carbon.

Catalyst ex-situ sulfiding. For the purpose of analysis, some catalysts were sulfided in all glass atmospheric pressure equipment which allows one to isolate the sulfided sample without exposure to air for further analysis. These sulfided samples will be referred to as *ex-situ* sulfided. Experimental conditions were 2 g of catalyst, H_2/H_2S (15%), flow rate = 40 ml/h, 400°C, 2 h, and temperature ramp = 5°C/min. Following the sulfiding step, samples were cooled to room temperature and then purged in purified helium at a flow rate of 40 ml/min at 50°C before being transferred into a cell sealed by means of two Teflon stopcocks.

Catalyst characterization. The metal content of the prepared and used catalysts were measured by X-ray fluorescence (XRF) using a Philips PW 1404 or 1480 apparatus. The BET surface areas of the oxides and used samples were determined using Micromeritics ASAP 2000 equipment. BET surface area values are reported in Table 1 except for the Ru catalyst which was not calcined. The radial distributions of the metals in the grains were measured by electron probe microanalysis (EPMA) with a Camebax electron microprobe. EPMA radial concentration profiles were found homogeneous for all oxide precursors, except for Ru showing a weakly pronounced U-shaped radial concentration profile.

X-ray diffraction (XRD) analysis was carried out on a SIEMENS D500 diffractometer equipped with a molybdenum target and a primary beam monochromator ($\lambda = 0.709$ Å), in transmission focusing geometry. Tested samples were protected against oxidation by a sealed polyethylene film and transferred under helium from the glove bag to the spectrometer. The low-angle scattered and diffracted signal from the polyethylene ($2\theta < 12.5°$) is not shown in the diffractograms.

Conventional TEM images were recorded to evaluate changes in the morphology of the observed sulfide particles in the used catalysts samples. This was done using a JEOL 100 CX instrument. Samples were recovered wet from the reactor and transferred to a glove bag. *Ex-situ* sulfided samples prepared in a cell were opened in the glove bag. The samples were put on a grid in *n*-heptane to avoid contact of the surface with air and were transferred to the microscope. To ensure a representative sampling of the particles morphology, at least ten images were recorded per sample and several hundred particles were counted and measured unless otherwise stated.

RESULTS

The catalysts prepared in this work were tested for the HYD of CHE, the HDS of BT, and the HDS of DBT after being sulfided under the same conditions. The activities are reported in Table 3 in terms of rate per gram of catalyst both in the case of transformation of the reactant into products ($r_{w,trans}$), or true hydrogenation ($r_{w,hyd}$), or true hydrodesulfurization ($r_{w,hds}$). The choice of reactants was made to be able to compare different functionalities of the active phases while trying to keep similar reaction conditions, especially reaction temperature and pressure. After preliminary tests it appeared that the HYD of CHE and the HDS of BT could be determined at 250°C and 6 MPa total pressure. On the other hand, most catalysts studied in this work were found inactive at 250°C for the HDS of DBT and therefore this reaction was performed at 350°C and 6 MPa. At this reaction temperature, the Mo catalyst was found so active that even the largest LHSV that could be employed with our equipment did not allow us to measure the activity. Therefore, for the Mo catalyst, DBT HDS activity measurements were made at different reaction temperatures, ranging from 280 to 320°C, and the activity at 350°C was obtained by extrapolation using a measured apparent activation energy of 120 kJ/mol.

TABLE 3

Activities of the Catalysts

Catalysts	Cyclohexene HYD (250°C, 6 MPa) LHSV (h^{-1})	$r_{w,trans}$[a]	$r_{w,hyd}$[a]	Benzothiophene HDS (250°C, 6 MPa) LHSV (h^{-1})	$r_{w,trans}$[a]	$r_{w,hds}$[a]	Dibenzothiophene HDS (350°C, 6 MPa) LHSV (h^{-1})	$r_{w,trans}$[a]	$r_{w,hds}$[a]
Mn	3	1.0	0.09	1	0.02	0.015	1	0.03	0.03
Fe	6	0.88	0.54	1	0.23	0.034	1	0.14	0.12
Zn	3	0.47	0.009	1	0	0	1	0.01	0.01
Cu	3	0.65	0.285	1	0.23	0.011	1	0.04	0.03
Ni	3	2.52	1.72	1	0.25	0.060	1	0.13	0.12
Ru	12	3.20	1.76	6	0.98	0.096	12	0.88	0.64
Mo	12	8.6	7.40	8	2.45	0.24	24	1.71[b]	1.28[b]
Re	3	4.03	3.16	4	0.75	0.19	4	0.6	0.53

[a] In mmol/g of catalyst/h. trans, transformation of reactant; hyd, hydrogenation; hds, hydrodesulfurization.
[b] Extrapolated from the results at 300°C.

From Table 3 it appears that on a gram of catalyst basis the Mo catalyst is the most active catalyst for all three reactions. Ru, Re, and in some cases Ni belong to a second group of moderately active catalysts, whereas Mn, Fe, Zn, and Cu are poorly active catalysts.

A number of elemental and standard physico-chemical analyses were performed to determine if these differences in catalytic properties resulted from the loss of metal, deactivation by coking, etc. In addition, as we are dealing with supported sulfide catalysts, it is better to compare catalytic activity on a moles of sulfided metal basis. Therefore, it was necessary to determine the actual amount of sulfided metal in the used catalysts.

The BET surface areas showed no major change compared to those of the oxide precursors (41). XRF analysis reported in Table 4 indicated no loss of metal content during the test in all of the studied catalysts except for Zn with a 50% loss. All used catalysts contained a small amount of carbon, less than 3 wt% except for the Zn catalyst with 5.5 wt% C. The sulfided alumina carrier contained about 1% of C and almost no sulfur. Therefore, in the following, deactivation by carbon deposits will not be considered to be a factor explaining the activity results.

In Table 4, S/metal molar ratios were computed from the metal and sulfur contents measured by XRF assuming that all of the sulfur is contained in the metal sulfide phase, a sound hypothesis as only a very small amount of sulfur is retained by the alumina after sulfiding.

XRD spectra of used catalysts were also recorded to identify the supported sulfide phase. No features except γ-alumina were detected for sulfided Ni, Mo, Ru, and Re catalysts using XRD. In contrast, Mn, Fe, Cu, and Zn catalysts showed well-defined features in their XRD spectra, allowing for the nature of the sulfide phase to be identified and particle size to be estimated. These results are reported in Table 5.

In Fig. 1, the XRD spectra of the Fe catalyst shows the presence of a well-crystallized $Fe_{1-x}S$ phase with a particle size of about 170 Å. XRD analysis of an *ex-situ* sulfided Fe

TABLE 4

Metals, Sulfur, and Carbon Contents of Used Catalysts

Catalysts	Metal (wt%)	S (wt%)	C (wt%)	S/metal (theo)[a]	S/metal (used) (XRF)	τ (% sulfur)
Alumina	0	Trace	1.1			
Mn	5.1	2.9	1.7	1	0.97	97
Fe	5.3	2.4	1.3	1	0.79	79
Zn	3.4	0.4	5.5	1	0.24	24
Cu	6.2	1.5	0.5	0.5	0.48	96
Ni	5.9	1.7	0.8	0.66	0.53	80
Ru	8.4	1.8	1.0	3	0.68	22
Mo	8.2	4.4	1.4	2	1.61	80
Re	10.4	1.9	0.7	2	1.06	53

[a] Ni_3S_2, FeS, Cu_2S, MnS, ZnS, MoS_2, RuS_{2+x} ($x = 1$), and ReS_2.

TABLE 5

Sulfide Phase Detected by XRD and TEM in Used Sulfided Catalysts

Catalysts	Sulfide form (XRD)	Particle size range (Å) (XRD)	Particle shape (TEM)	Particle size range (Å) (TEM)	Mean particle size (Å) (TEM)	M_{Fe}/M
Mn	MnS	320	nm	nm	nm	0.05
Fe	$Fe_{1-x}S$	170	Needle	45 × 200 120 × 600	nm	0.09
Zn	ZnS	100	nm	nm	nm	0.15
Cu	$Cu_{2-x}S$	120	Sphere	10–150	nm	0.12
Ni	nd	nd	Sphere	12–45	25	0.39
Ru	nd	nd	Sphere	10–40	20	0.39
Mo	nd	nd	Slabs	10–80	26	0.25
Re	nd	nd	Sphere	10–40	16	0.41

Note. nd, not detected; nm, not measured.

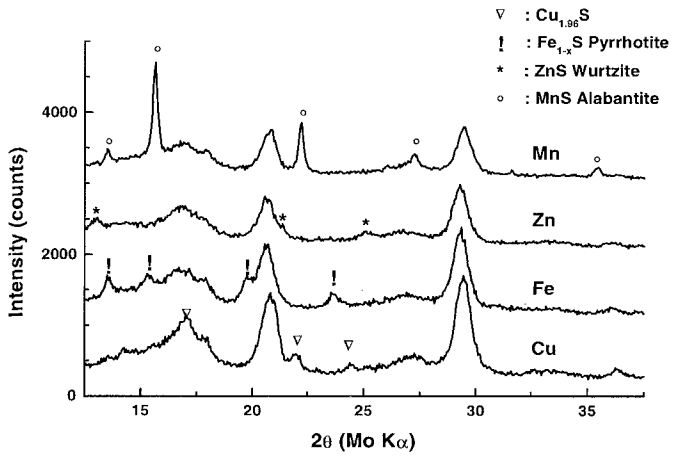

FIG. 1. XRD spectra of Fe, Cu, Mn, and Zn used catalysts.

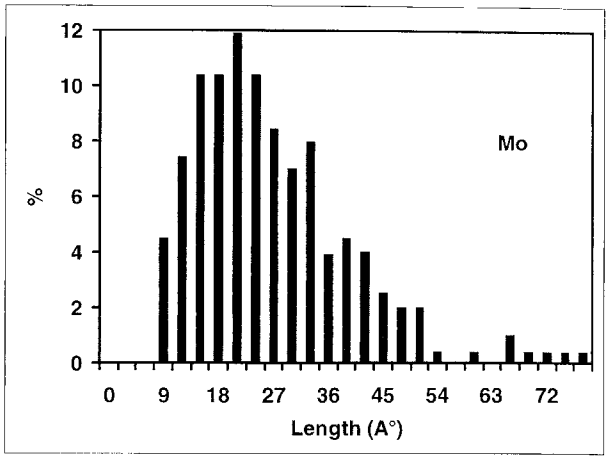

FIG. 2. Histogram of molybdenum sulfide particle size distribution in a used Mo catalyst.

catalyst confirmed this result and suggested the formation of the Fe_9S_{11} phase. The Cu catalyst contained crystallized $Cu_{2-x}S$ with a particle size of 120 Å (Fig. 1). This is in line with the detection of a $Cu_{2-x}S$ phase in a Cu/Al_2O_3 catalyst with 90% of the Cu sulfided as reported by Mangnus *et al.* using TPR (42). *Ex-situ* sulfiding of the Cu/Al_2O_3 catalyst led to a XRD spectra close to that of the anilite Cu_7S_4 phase, a phase stable at high temperature (43). Well-defined MnS crystallites were identified by XRD in the Mn catalyst with a particle size of about 320 Å (Fig. 1). *Ex-situ* sulfiding of the Mn catalyst confirmed the formation of 250-Å MnS particles. In both cases, particles of Mn_2O_3 detected in the oxide precursor had completely disappeared. MnS particles were previously identified in a bulk catalyst (1), on a carbon support (4), and proposed on alumina (42) from TPR results. ZnS crystallites were clearly identified in the Zn catalyst with a particle size of about 100 Å (Fig. 1). *Ex-situ* sulfiding of the Zn catalyst confirmed the formation of ZnS particles.

TEM analysis of sulfided Ni, Mo, Ru, Re, Fe, and Cu samples was then undertaken to estimate the mean particle sizes of the sulfide phases. No TEM analyses were performed for a Mn- and Zn-based catalyst in view of their very low activity and the detection of well-crystallized particles by XRD. Nickel sulfide particles in the Ni catalyst were observed with difficulty in the TEM pictures. Detected particles appear mostly spherical with a particle size in the range 12–45 Å. Although is was not possible to count a large number of particles to establish a detailed histogram for particle size distribution, a mean size of 25 Å was roughly estimated.

For the Mo catalyst, TEM pictures showed well-dispersed particles containing one or two MoS_2 layers. The histogram of the molybdenum sulfide particle size distribution of the Mo catalyst presented in Fig. 2 indicates that the length of the layers varies from 8 to 80 Å with a mean value of 26 ± 3 Å. In very few cases large particles, 400–1300 Å, composed of a core surrounded by a small MoS_2 layer of 30 Å were observed. This is usually attributed to reduced MoO_3 particles surrounded by MoS_2.

Spherical, homogeneously dispersed, Ru sulfide particles were clearly visible on the TEM pictures of the Ru catalyst. The histogram in Fig. 3 shows a ruthenium sulfide particle size from 10 to 40 Å with a median diameter of 20 Å.

On the Re catalyst, numerous homogeneously dispersed spherical particles were detected by TEM with a particle size in the range 10–21 Å and a median diameter around 16 Å (Fig. 4). It is assumed that these particles are ReS_2, which has been reported for bulk Re sulfide (1), sulfided Re on carbon (8) and that on silica (20). Re_2S_7 is also reported to transform rather easily into ReS_2 (43).

The Fe catalyst particles were difficult to count and therefore no attempt has been made to establish a particle size distribution. On the Fe catalyst large needle-like particles from 45×200 to 120×600 Å were found and assigned to

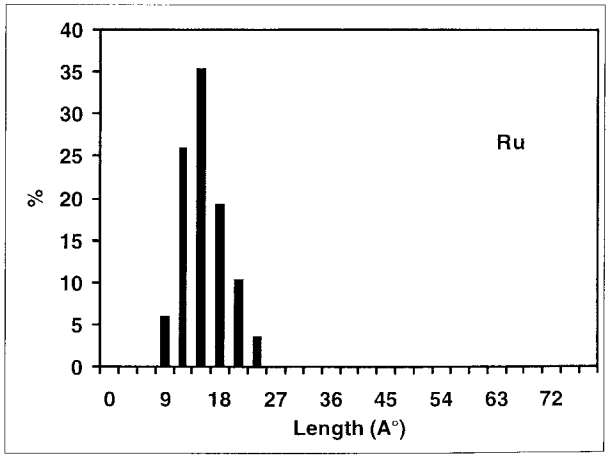

FIG. 3. Histogram of ruthenium sulfide particle size distribution in a used Ru catalyst.

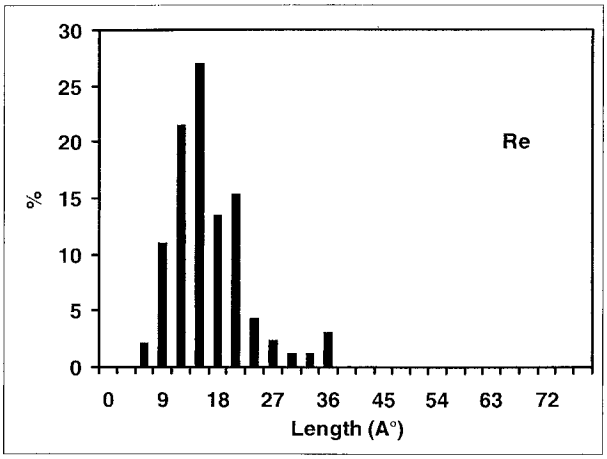

FIG. 4. Histogram of the Re sulfide particle size distribution in a used Re catalyst.

the hydrated iron sulfate phase. The differences in particles sizes between TEM and the XRD could be due to partial oxidation of the iron sulfide phase or to defects in the structure. The Cu catalyst contains ill-defined but homogeneously dispersed copper sulfide particles in the Cu catalyst with a size ranging from 10 to 150 Å.

While XRD allowed us to identify the MnS, FeS, Cu_2S, and ZnS sulfide phase of Mn, Fe, Cu, and Zn catalysts, it was assumed that the main sulfide phases were Ni_3S_2, RuS_2, MoS_2, and ReS_2 for Ni, Ru, Mo, and Re catalysts, respectively. In the case of the Ru catalyst, however, it has been reported that the actual S/Ru ratio of an alumina-supported catalyst is usually closer to 3 than 2 (26, 27, 44). This is assumed to be due to the coverage of the surface of the tiny RuS_2 particles by surface S_2^{2-} groups (45). Therefore, for the Ru catalyst a theoretical S/Ru ratio of 3 is assumed for the computation of the amount of sulfided Ru in the catalyst.

The measured S/metal molar ratio can then be compared to the reference S/M ratio to estimate the sulfiding degree of the metal. The values reported in Table 4 indicate that the Ni, Mo, Fe, Cu, and Mn catalysts are rather well sulfided, Re is half sulfided, and Ru and Zn are poorly sulfided. Several reasons can be advocated to understand the low sulfiding degree of Re, Ru, and Zn, such as the presence of a metallic phase for Ru and Re and the incorporation of the cation in the alumina surface layer for Zn. Using the sulfiding degree of the metals, the activities per mole of sulfided metal were computed according to Eq. [3] for the three reactions performed and reported in Fig. 5.

DISCUSSION

The activities for the HDS of DBT of alumina-supported sulfides measured in this work were first compared to the activities reported for bulk sulfides by Pecoraro and Chianelli (1). In Fig. 6, a very nice similarity is found between the two sets of results except that in Pecoraro and Chianelli's work Ru sulfide was considerably more active than Mo and Re sulfide. This indicates that the alumina support has no major effect on the shape and position of the volcano curve.

In Fig. 5A, the activities for the transformation of the three compounds, CHE, BT, and DBT per mole of sulfided metal can be compared in the form of histograms. The Mn, Fe, Zn, Cu, and Ni catalysts are definitely much less active than the Mo, Ru, and Re catalysts, whatever the catalytic reaction considered. The Mo, Ru, and Re catalysts have activities of the same order of magnitude. However, the Re and Mo catalysts are more active than Ru for CHE HYD with the activity ranking Ru < Mo < Re, Re is more active than Ru for BT HDS with the activity ranking Mo < Ru < Re, and Ru is the most active catalyst for DBT HDS with the activity ranking Re < Mo < Ru.

One major source of uncertainty in this comparison of sulfided catalysts activities is the actual sulfiding degree of the metals and in particular Ru. We have chosen a theoretical value of S/Ru = 3 to evaluate the sulfiding degree of Ru. If a value of 2 had been chosen, Ru would have been slightly less active than the Mo catalyst. On the other hand, experimental data reporting a S/Ru ratio of more than 3 have been reported in the literature (26–28, 36, 44). If a value of 4 for the S/Ru had been chosen, then the sulfiding degree of the Ru in our catalyst would have been lower and the activity per sulfided Ru higher.

The low sulfiding degree of Ru in our catalyst could be explained by inadequate sulfiding conditions for the Ru catalyst as all of the catalysts have been sulfided in the testing unit using a toluene/cyclohexane/dimethyldisulfide mixture under hydrogen pressure. Such a sulfiding method is not favorable for the Ru and Re catalyst as indicated by the low degree of sulfiding reached, namely, 22% for the Ru catalysts and 53% for the Re catalyst. Note that studies of

TABLE 6

Geometrical Model of Sulfide Particles

	Mo, MoS_2 slab model (46)	Ru, cfc particle (45)	Mn, Fe, Zn, Cu, Ni, Re Cubic crystal model
M_t	$3n^2+3n+1$	$4n^3+6n^2+3n+1$	$(n+1)^3$
M_{surf}	$6n+12$	$12n^2+2$	$6n^2+2$
M_c	6	8	8
M_v	$6n+12$	$12n-4$	$12n-4$
M_{fe}	$6n+6$	$12n^2-12n+6$	$6(n-1)^2$

Note. n = number of metal pairs on one side of the crystallite, M_t = total number of metal atoms in the crystallite, M_c = number of corner metal sites, M_{surf} = number of surface atoms (including corners), M_v = number of vertices atoms (including corners), and M_{fe} = number of edge metal sites in MoS_2 (corner not included) or the number of external surface sites for other sulfides (corner and vertice sites not included).

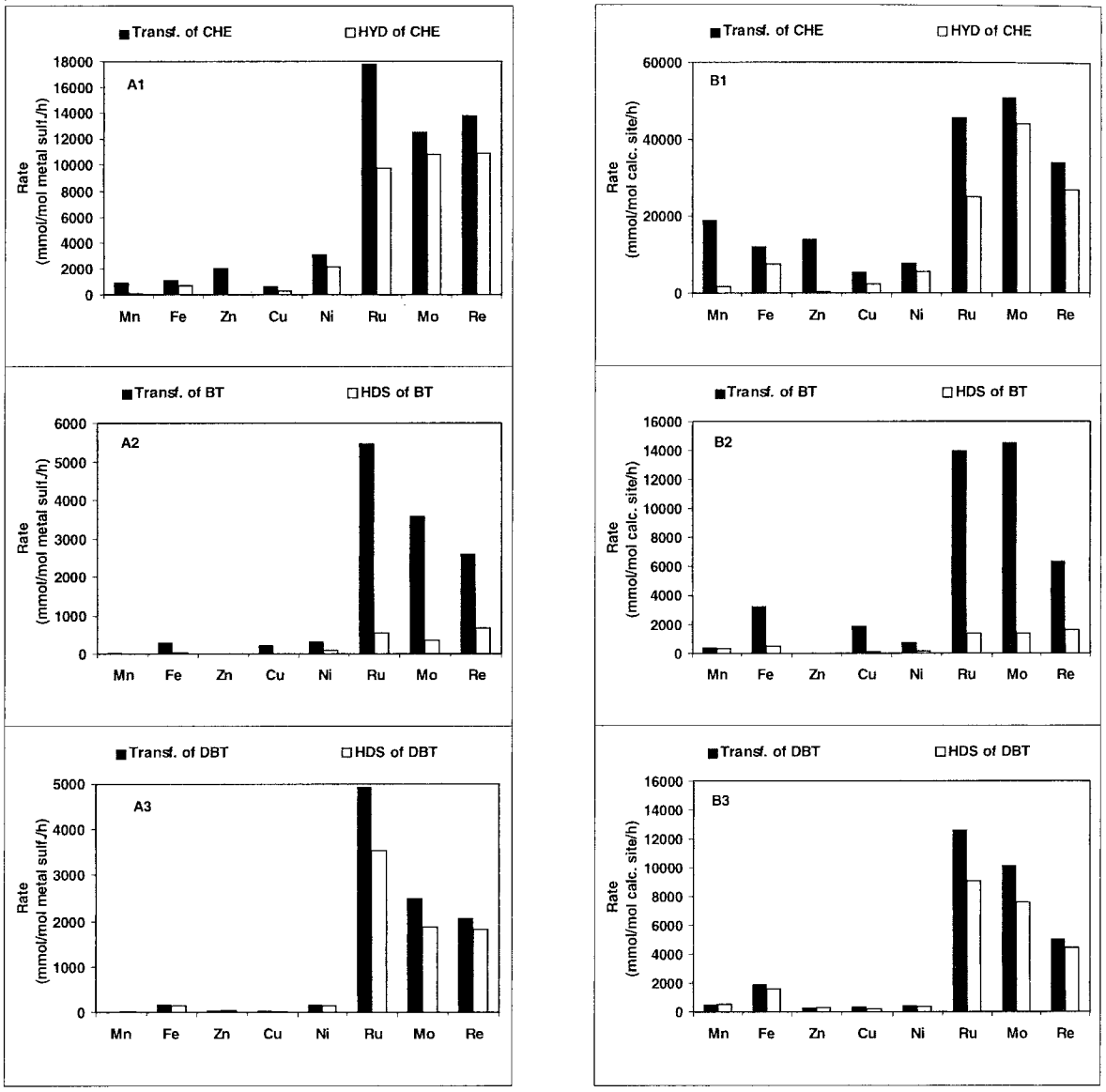

FIG. 5. Catalytic activities for (1) cyclohexene hydrogenation, (2) benzothiophene hydrodesulfurization, and (3) dibenzothiophene hydrodesulfurization of Mn, Fe, Cu, Zn, Ni, Ru, Mo, and Re catalysts listed according to their increasing M–S bond energy (1, 29). (A1, A2, A3) Activities per mol of metal sulfide; (B1, B2, B3) activities per mol of calculated sites (see text).

gas-phase sulfiding of Ru catalysts at atmospheric pressure have shown that a N_2/H_2S mixture is better than a H_2/H_2S mixture (44). However, with our equipment such a method could not be employed.

A truly significant comparison of the activity of sulfides should evidently be made using the activity per site. However, a measurement of the number of sites of sulfides is not available at the present time. Therefore, one can attempt to estimate the influence of the catalyst particle morphology by using geometrical models such as those developed for MoS_2-based catalysts (46) and RuS_2-based catalysts (45). An estimation of the geometrical number of sites has been performed in this work by using the aforementioned geometrical models for Mo and Ru sulfides. For the sake of simplicity, a cubic particle model was used for the Mn, Fe, Zn, Cu, Ni, and Re sulfides. The formulae giving the total number of metal atoms (M_t) as well as the number of supposedly active metal centers on the external planes of the sulfide crystallites (excluding corners and vertices), hereafter called face/edge (M_{fe}) atoms, are reported in Table 6 for the MoS_2 hexagonal slab model (46), the RuS_2 cfc particle model (45), and the cubic particle model. When the amount of sulfided metal as well as a mean particle size determined from TEM or XRD, was used, an estimate of the geometric number of sites per gram of catalyst was made. Computed values of M_{fe}/M are reported in Table 5

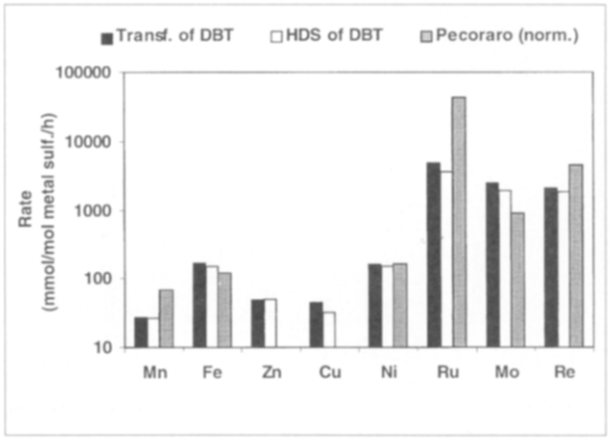

FIG. 6. DBT HDS catalytic activities of TMS per mol of metal sulfide. Bulk sulfides activities are taken from Pecoraro and Chianelli (1) and were normalized relative to Ni.

and show that the variation is less than an order of magnitude. In addition, the M_{fe}/M correcting factor is not very different for Ru, Re, and Mo, whereas it is more important for large sulfide particles like MnS, CuS, and FeS. Therefore, the activity per calculated site reported in the form of a histogram in Fig. 5B does not show major differences with those reported in Fig. 5A. Again, whatever the reaction, the activity rankings reveal two groups of alumina-supported sulfides, the low-reactivity group with Mn, Fe, Zn, Cu, and Ni and the high-activity group with Ru, Mo, and Re. A comparison of the activity per calculated site and the activity per mole of sulfided metal reveals only small changes of activity ranking. In addition, Fig. 5B shows that the difference in terms of activity per calculated site is no longer important between Ru, Re, and Mo catalyst.

These comparisons indicate, however, that one must be cautious when comparing activities of various supported metal sulfides because the actual amount of sulfided metal and the particle dispersion must be taken into account. More precise measurements of the number of sites are therefore required to reach a definite conclusion about the activity ranking of these sulfides.

CONCLUSION

This study has shown that a typical volcano curve is obtained for the DBT HDS activity of alumina-supported Mn, Fe, Zn, Cu, Ni, Ru, Mo, and Re sulfides versus metal–sulfur bond energy, which compares well with the volcano curve reported for bulk sulfides by Pecoraro and Chianelli. In both cases Ru sulfide is the most active sulfide. The alumina support has therefore no effect on the existence of the volcano curve for DBT HDS.

The trends found for cyclohexene hydrogenation and benzothiophene HDS were different from the DBT HDS trend and both depend on whether the transformation of the reactant or the actual hydrogenation or hydrodesulfurization is taken into consideration. Therefore, on alumina the sulfide activity trends versus metal–sulfur bond energy were found to depend on the nature of the catalytic reaction performed.

The catalytic activities of alumina-supported Mn, Fe, Zn, Cu, and Ni sulfides were very low whereas those of alumina-supported Ru, Mo, and Re sulfides were high, whatever the reaction performed. These results were established for catalytic activities per mole of metal sulfided which took into account the sulfiding degree of the catalysts as in our experimental conditions Ni, Mo, Fe, Cu, and Mn catalysts were well sulfided, Re was half sulfided, and Ru and Zn were poorly sulfided. An attempt to evaluate and take into account a geometrical number of sites does not lead to major changes in the activity ranking of the various sulfides studied in this work.

ACKNOWLEDGMENTS

We are indebted to Dr. P. Raybaud for making available to us the computed metal–sulfur bond energy for CuS and ZnS. The work performed by the staff of the Physico-chemical and Analytical Department of IFP is gratefully acknowledged. More specifically, the authors wish to acknowledge the contributions of Bernadette Rebours, Eliane Leplat, and Karine Esterlé.

REFERENCES

1. Pecoraro, T., and Chianelli, R. R., *J. Catal.* **67**, 430 (1981).
2. Lacroix, M., Boutarfa, N., Guillard, C., Vrinat, and M., Breysse, M., *J. Catal.* **120**, 473 (1989).
3. Lacroix, M., Marrakchi, H., Calais, C., Breysse, M., and Forquy, C., *Stud. Surf. Sci. Catal.* **59**, 277 (1991).
4. Vissers, J. P. R., Groot, C. H., van Oers, E. M., de Beer, V. H. J., and Prins, R., *Bull. Soc. Chim. Belg.* **93**, 813 (1984).
5. Ledoux, M. J., and Djellouli, B., *J. Catal.* **115**, 580 (1989).
6. Eijsbouts, S., de Beer, V. H. J., and Prins, R., *J. Catal.* **109**, 217 (1988).
7. Eijsbouts, S., de Beer, V. H. J., and Prins, R., *J. Catal.* **127**, 619 (1991).
8. Ledoux, M. J., Michaux, O., Agostini, J., and Panissod, P., *J. Catal.* **102**, 275 (1986).
9. Raje, A. P., Liaw, S. J., Srinivasan, R., and Davis, B. H., *Appl. Catal. A: Gen.* **150**, 297 (1997); *Appl. Catal. A:* **150**, 319 (1997); *Appl. Catal. A: Gen.* **150**, 343 (1997).
10. Sudhakar, C., Eijsbouts, S., de Beer, V. H. J., and Prins, *R. Bull. Soc. Chim. Belg.* **96**, 885 (1987).
11. Shabtai, J., Guohe, Q., Balusami, K., Nag, N. K., and Massoth, F. E., *J. Catal.* **113**, 206 (1988).
12. Wakabagashi, K., and Orito, Y., *Kogio Kagatu Zashi* **74**, 382 (1971).
13. Shabtai, J., Nag, N. K., and Massoth, F. E., *J. Catal.* **104**, 413 (1987).
14. Dhainaut, E., Charcosset, H., Gachet, C., and de Mourgues, L., *Appl. Catal.* **2**, 75 (1982).
15. Navarro, B., Pawelec, B., Fierro, J. L. G., Vasudevan, P. T., Cambras, J. F., and Arias, P. L., *Appl. Catal. A: Gen.* **137**, 269 (1996).
16. Vissers, J. P. R., de Beer, V. H. J., and Prins, R., *Prepr. Am. Chem. Soc., Div. Petrol. Chem.* **32**, 347 (1987).
17. Breysse, M., Afonso, J., Lacroix, M., Portefaix, J. L., and Vrinat, M., *Bull. Soc. Chim. Belg.* **100**, 923 (1991).
18. Ternan, M., *J. Catal.* **104**, 256 (1987).
19. Vit, Z., and Zdrazil, M., *J. Catal.* **119**, 1 (1989).

20. de Los Reyes, J. A., Vrinat, M., Geantet, C., and Breysse, M., *Appl. Catal. A: Gen.* **103**, 79 (1993).
21. Liaw, S. J., Raje, A. P., Lin, R., and Davis, B. H., *Prepr. Am. Chem. Soc., Div. Petrol. Chem.* **39**, 636 (1994).
22. de Los Reyes, J. A., Vrinat, M., Geantet, C., and Breysse, M., *Catal. Today* **10**, 645 (1991).
23. Vrinat, M., Lacroix, M., Breysse, M., Mosoni, L., and Roubin, M., *Catal. Lett.* **3**, 405 (1989).
24. Mitchell, P. C. H., and Scott, C. E., *Bull. Soc. Chim. Belg.* **93**, 619 (1984).
25. de Los Reyes, J. A., Göbölös, S., Vrinat, M., and Breysse, M., *Catal. Lett.* **5**, 17 (1990).
26. Kuo, Y. J., and Tatarchuk, B. J., *J. Catal.* **112**, 229 (1988).
27. Kuo, Y. J., Cocco, R. A., and Tatarchuk, B. J., *J. Catal.* **112**, 250 (1988).
28. Lu., K., and Tatarchuk, B. J., *J. Catal.* **116**, 166 (1987).
29. Toulhoat, H., Raybaud, P., Kasztelan, S., Kresse, G., and Hafner, J., *Catal. Today* **50**, 629 (1999).
30. Raybaud, P., personnal communication
31. Karroua, M., Ladrière, J., Matralis, H., Grange, P., and Delmon, B., *J. Catal.* **138**, 640 (1992).
32. Mitchell, P. C. H., Scott, C. E., Bonnelle, J. P., and Grimblot, J., *J. Catal.* **107**, 482 (1987).
33. Le Page, J. F., *et al.*, "Catalyse de Contact." Technip, Paris, 1976.
34. Vrinat, M. L., *Appl. Catal.* **6**, 137 (1983).
35. Girgis, M. J., and Gates, B. C., *Ind. Eng. Chem. Res.* **30**, 2021 (1991).
36. Odebunmi, E. O., and Ollis, D. F., *J. Catal.* **80**, 65 (1983).
37. Nag, N. K., Sapre, A. V., Broderick, D. H., and Gates, B. C., *J. Catal.* **57**, 509 (1979).
38. Ishihara, A. T., Itoh, T., Hino, T., Nomura, M., Qi, P., and Kabe, T., *J. Catal.* **140**, 184 (1993).
39. Broderick, D. H., and Gates, B. C., *AIChE J.* **27**, 663 (1981).
40. Singhal, C. H., Espino, R. L., and Sobel, J. E., *J. Catal.* **67**, 446 (1981).
41. Quartararo, J., Ph.D. thesis, Université Paris VI, 1996.
42. Mangnus, P. J., Riezebos, A., van Langeveld, A. D., and Moulijn, J. A., *J. Catal.* **151**, 178 (1995).
43. Nickless, G., *in* "Inorganic Sulfur Chemistry" (G. Nickleso, Ed.). Elsevier, Amsterdam, 1968.
44. de Los Reyes, J. A., Vrinat, M., Geantet, C., Breysse, M., and Grimblot, J., *J. Catal.* **142**, 455 (1993).
45. Geantet, C., Calais, C., and Lacroix, M., *C. R. Acad. Sci. Paris, ser. II* **315**, 439 (1992).
46. Kasztelan, S., Toulhoat, H., Grimblot, J., and Bonnelle, J. P., *Appl. Catal.* **13**, 127 (1984).